A COLLINEAR WAKEFIELD ACCELERATOR FOR A HIGH REPETITION RATE MULTI BEAMLINE SOFT X-RAY FEL FACILITY*

A. Zholents #, W. Gai, R. Lindberg, J.G. Power, Y. Sun, ANL, Argonne, IL 60439, USA
C. Jing, A. Kanareykin, Euclid Techlabs LLC, Solon, OH 44139, USA
C. Li, C.X. Tang, Tsinghua University, Beijing, China
D. Yu. Shchegolkov, E.I. Simakov, LANL, Los Alamos, NM 87545, USA

Abstract

A concept is presented for a multi beamline soft x-ray free-electron laser (FEL) facility where several FEL undulator lines are driven by an equal number of high repetition rate single-stage collinear wakefield accelerators (CWA). A practical design of the CWA, extending over 30 meters and embedded into a quadrupole wiggler, is considered. The wiggler's structure of alternating focusing and defocusing quadrupoles is used to control single-bunch breakup instability. It is shown that practical restrictions on the maximum attainable quadrupole field limit the maximum attainable charge in the drive bunch whose sole purpose is to produce a high accelerating field in the CWA for the following main bunch. It is also pointed out that the distance between drive and main bunches varies along the accelerator, causing a measurable impact on the energy gain by the main bunch and on the energy spread of electrons in it. Means to mitigate these effects are proposed and results are presented for numerical simulations demonstrating the main bunch with plausible parameters for FEL application including a relatively small energy spread. Finally, results are presented for the expected FEL performance using an appropriately chosen undulator.

INTRODUCTION

A number of FEL facilities are currently in operation [1-4] and more have been planned. While tremendously effective in providing extreme photon fluxes, these machines can only accommodate a small number of users at a time. To address this limitation, multi-user FEL facilities have been recently proposed (see, for example, [5]). The mainstream approach is to accelerate electron bunches in a few GeV cw superconducting rf (SRF) linac and send them to a switchyard of ten or more FELs at a high bunch repetition rate. Here, we consider a different approach where a single cw SRF linac of a much lower energy (~400 MeV) and ten CWAs are used to provide ten FELs with a few GeV electron bunches. It is expected that the construction and operational costs of the facility, which are largely defined by the large SRF linac, can be significantly reduced. A high-gradient room-temperature CWA structure is the key to this proposal. Advanced accelerator studies aimed at a future high-energy collider have shown impressive results, achieving multiple-GV/m energy gradients in various wakefield acceleration schemes [6,7].

*Work supported by U.S. Department of Energy, Office of Science, under Contract No. DE-AC02-06CH11357 and by the U.S. Department of Energy through the Laboratory Directed Research and Development (LDRD) program at Los Alamos National Laboratory.
#azholents@aps.anl.gov

A CWA SCHEME FOR FEL

In a collinear wakefield accelerator [8,9], the field generated by a leading, high-charge drive bunch is used to accelerate a trailing low-charge main bunch. The collinear configuration has the two beams traversing the accelerator along the same trajectory so that the energy is directly transferred from the drive bunch to the main bunch. There are two main candidates for a CWA structure. The corrugate pipe wakefield accelerator (CPWA) [10] structure consists of a metallic pipe with wall corrugations where traveling on the pipe's axis relativistic electrons excite a synchronous monopole mode whose amplitude and frequency is defined by the pipe radius and geometry of corrugations. The dielectric wakefield accelerator (DWA) [11] structure consists of a cylindrical dielectric tube with an axial vacuum channel inserted into a copper outer jacket. The dielectric constant and the inner and outer radii of the dielectric tube are chosen to adjust the fundamental monopole mode (TM_{01}) frequency excited by the relativistic electrons. The phase velocity of the mode equals the beam velocity ~c.

The overall facility layout is shown in Figure 1. The scheme consists of 10 parallel FELs and ten parallel CWAs that supply FELs with a ~ 2 GeV electrons. The CWAs share a single 650 MHz cw SRF linac that accelerates 8-nC drive and 250-pC main bunches to ~400-MeV. Because of a need for the tight synchronization between drive and main bunches (of the order of 250 fs), both bunches are obtained from one source bunch as discussed below. The repetition rate of duets of drive and main bunches in the CWA is limited to ~ 50 kHz. This keeps the average wakefield power dissipation in the accelerating structure at a manageable level, as shown later. Thus, the bunch repetition rate in the cw SRF linac is ~500-kHz. A spreader switchyard distributes electron bunches to the ten CWAs on a rotating basis (or as needed). The drive bunch has a special double triangular current profile, shown in Figure 2. The bunch current shape is tailored to maximize the transformer ratio R, defined as the ratio of the maximum accelerating field behind the drive bunch over the maximum decelerating field inside the bunch. Obtaining short drive bunch ~ 3.3 ps requires off-crest acceleration of the already pre-shaped bunch in SRF linac producing ~ 10% energy chirp

ISBN 978-3-95450-133-5

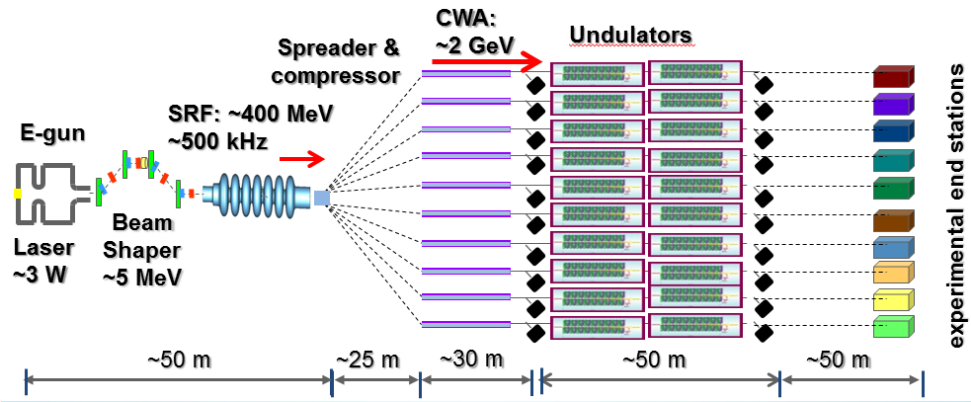

Figure 1: A schematic of the FEL facility showing (not to scale) an electron gun, bunch shaping section, cw superconducting linac, spreader and transport lines, an array of collinear wakefield accelerators, undulator arrays, and x-ray beamlines.

at the end and ~ a tenfold bunch compression in each spreader beam line. The energy chirp that remains after the compression assists in suppression of single-bunch breakup instability as discussed later in this paper.

The effective acceleration length of the CWA is ~30 m, over which distance the drive bunch loses ~80% of its energy and the main bunch gains ~ 1.6 GeV. As presently considered, each CWA has 40 half-meter-long acceleration sections followed by shorter break sections that include beam diagnostics, vacuum ports and a THz frequency directional coupler. In the case of the DWA, the vacuum chamber of the acceleration section consists of a quartz-based tube with copper cladding. A ceramic with DC conductivity [12] will be used in the dielectric layer allowing discharging of the erroneous charges produced by the electromagnetic showers induced by stray electrons. The inner surface can also be coated by a few nanometer metallic or TiN layer [13]. Cooling is provided to remove the heat load produced by the wakefields which is calculated to be 10.8-W per cm of a linear length of the DWA structure for the Case 2 of beam parameters discussed below. This chamber is embedded into a quadrupole wiggler with soft-iron magnetic poles excited by permanent magnets, as shown in Figure 3. The same chamber can be used in the case of the CPWA except corrugations on the inner wall instead of the dielectric layer. The chamber has a small 2-mm diameter hole, essential for achieving a high acceleration gradient using CWA.

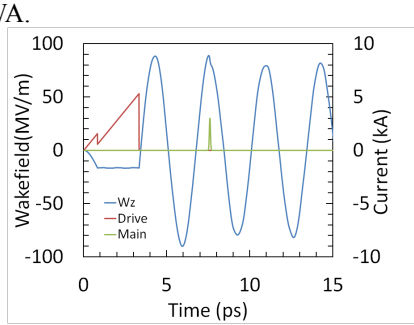

Figure 2: Drive bunch double triangle current profile and the wakefield due to drive and main bunches.

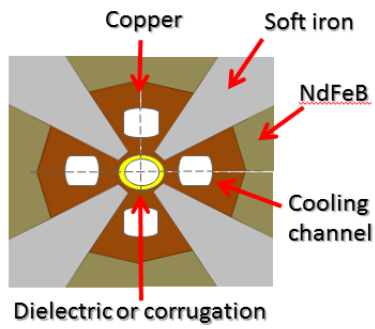

Figure 3: A cut-out part of the central area of the CWA showing the quadrupole wiggler and the vacuum chamber with cooling channels and either dielectric or corrugated inner part (marked by yellow colour). Electron beam propagates on the axis of the central cross.

DRIVE BUNCH SHAPING

The main plan for obtaining a double triangle current profile of the drive bunch is to use the mask with a special form shown in Figure 4. The same mask is also used to shape the low charge main bunch and fix it at a precisely defined distance behind the drive bunch.

The mask is placed in front of the transverse-to-longitudinal emittances exchange (EEX) beamline [14-21] which converts the red-coloured transverse image in Figure 4 into the double triangle longitudinal profile at the end of the beamline shown in Figure 2. The transmission efficiency of the mask is only ~45% and, therefore, we consider carrying out bunch shaping at a low beam energy ~5-MeV below a threshold energy for the material activation for copper. With a 500 kHz bunch repetition rate, approximately 25-kW of a source beam power is absorbed by the mask.

ISBN 978-3-95450-133-5

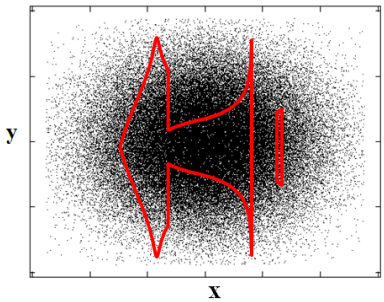

Figure 4: The outline of the mask boundary (red curve) on a background of Gaussian distribution of electrons of the source bunch in transverse coordinates [14].

A different approach is proposed in [22] where a near triangular bunch current profile is obtained using a combination of a wakefield producing dielectric tube and a compact magnetic chicane. It is therefore possible to use a double emittance exchange beamline [23] in order to convert the longitudinal profile obtained in [22] into the transverse distribution using the first emittance exchange leg, to apply the mask, and to use the second emittance exchange leg to convert the transverse distribution after the mask into the double triangle longitudinal profile at the end. Here, starting with the pre-shaped longitudinal distribution, the transmission efficiency of the mask is expected to be at ~80-90% level.

As discussed above, final compression of the drive and main bunches is planned after acceleration to 400 MeV utilizing the energy chirp acquired through bunch shaping manipulations and off-crest acceleration in the SRF linac and the spreader beamline beam transport time-of-flight properties.

A proof-of-principle experiment for beam shaping is in preparation at the AWA facility [24,25] with a 5-nC Gaussian bunch and plausible transverse and longitudinal emittances at 75 MeV electron beam energy.

MAIN PARAMETERS

Since physics of beam acceleration in CPWA and DWA is practically identical, we only discuss here the main beam parameters for a case of DWA. In order to inform design choices and evaluate sensitivities of the DWA to the key parameters of the dielectric channel and parameters of the drive and main bunches, we consider two hypothetical cases summarized in Table 1. The Case 2 is currently selected as our preferred scenario. In this case a ~90-MeV/m acceleration gradients is achieved at the wakefield maximum with the transformer ratio R =5 using a 8-nC drive bunch. A drive-beam-to-main-beam energy transfer efficiency is calculated to be ~ 15% using a 250-pC main bunch. All the values are calculated using four longitudinal structure modes, but the fundamental mode gives the dominant contribution because each structure is designed to minimize the loss factor of higher-order modes (HOMs). This is very important for achieving a high transformer ratio, as well as to mitigate the self-wakefield induced disturbances inside the main bunch as discussed later. Stable propagation of a drive bunch with energy varying from 400-MeV to 80-MeV along the CWA through this hole presents a significant challenge and is discussed later.

While the structure is optimized to maintain a single-mode excitation for the drive beam, multiple modes are excited by the main beam due to its shorter bunch length. But the self-wakefield inside the main bunch will converge very fast because the loss factor of HOMs becomes negligible beyond the first few modes. A 250-pC per bunch and 10-μm rms main bunch length were chosen in the design to allow a 3-kA peak current with a reasonable beam loading in the CWA.

Table 1: DWA and Beam Parameters

Parameter	Case 1	Case 2	Units
Fundamental mode frequency	400	300	GHz
ID/OD/Length	1.5/1.59/100	2,/2.12/100	mm
Drive bunch charge	3.5	8	nC
Drive bunch energy	300	400	MeV
Double triangular bunch length	1	1	mm
Peak acc. field	42	90	MV/m
Bunch rep. rate	100	50	kHz
Power dissipation without/with THz field coupler*	19/5.4	55/10.8	W
Transformer ratio	8	5	
Main bunch charge/length	50/5	250/10	pC/μm
Drive beam dump energy	70	80	MeV
Total DWA length	40	20	m
Drive-to-main beam efficiency	8.6	15.5	%
Main beam energy	1.9	2.0	GeV

* per unit length, 100% THz field coupling efficiency is assumed

BEAM BREAKUP INSTABILITY

The small aperture of the CWAs structures makes the drive bunch particularly vulnerable to the single-bunch breakup (BBU) instability predominantly driven by transverse HEM_{11} mode [26,27]. We consider using BNS damping [28] to control the BBU and, thus, surround the CWA by a quadrupole wiggler (composed of alternating focusing and defocusing quadrupole schematically shown in Figure 5) and use the energy chirp in the drive bunch entering the CWA.

ISBN 978-3-95450-133-5

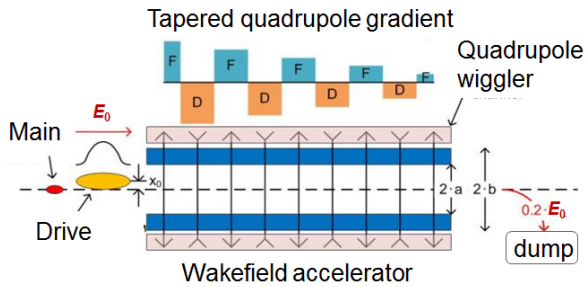

Figure 5: Schematic of a CWA. The quadrupole field is tapered to match the energy loss of the drive bunch along the accelerator. The final energy of the drive bunch at the end of the structure is 20% of its initial energy.

In order to better understand main parameter dependencies, we developed a simple two-particle model [29] that was later found to correctly represent the BBU for the drive bunch with a Gaussian longitudinal distribution. Using this model we determine the maximum achievable acceleration gradient as a function of the accelerating structure inner radius a shown in Figure 6. A grey area on this plot represents a stable region and a white area represents the unstable region. The border curve scales as $\sqrt{a}$ in a good agreement with results of multiparticle tracking shown by red circles. In this simple model, the ultimate extent of the stability region is limited by a maximum attainable strength for the quadrupole field (that in this study was scaled as a^{-1} from the value of 1-T/mm at a =1 mm). The dashed lines show scaling of the acceleration gradient when BBU is ignored.

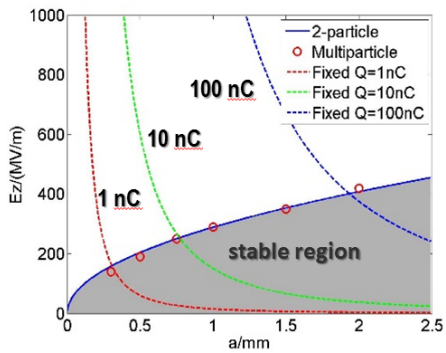

Figure 6: Maximum attainable energy gain in the CWA limited by BBU as a function of accelerating structure inner radius.

The remaining studies we did using the drive bunch with a double triangular current distribution. In this case when electrons lose much of their energy, the tail electrons begin to lag behind the head electrons to the extent that they even move into the region of the accelerating wakefield [30]. At the same time, the main bunch that gains a lot of energy begins to approach the tail of the drive bunch and goes out of the region with the maximum accelerating field. This effect is more pronounced when the drive's bunch energy is mostly used, and the energy of the tail electrons therefore becomes very low. One option to reduce relative slippage of drive and main bunches is to increase the energy of a drive bunch which has prompted us to use 400 MeV SRF linac.

Another technique to mitigate slippage of the drive and main bunches with respect to each other is to position the main bunch at the second maximum of the wake field behind the drive bunch. One can also increase the frequency of the wakefield along the dielectric channel—either by decreasing the tube's radius or thickness of the dielectric layer, or depth of corrugations — and keep the main bunch at or near the second wakefield maximum. Ideally, this wakefield frequency adaptive CWA will be insensitive to the main bunch shifts closer to the drive bunch during the acceleration.

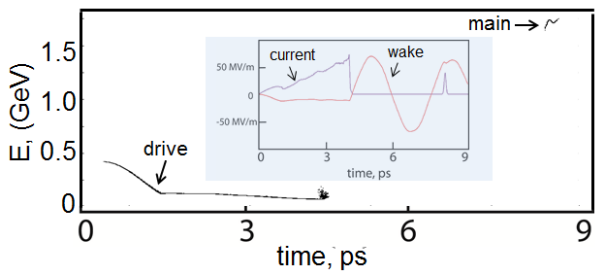

Figure 7: The result of the particle tracking showing energy variation in the drive and main bunches at a location of 18 m downstream of the DWA. The inset in the middle shows current in the drive and main bunches and the wakefield produced by the drive bunch with this current distribution.

The simulation result for the DWA with parameters given in Table 1 for the Case 2 is shown in Figure 7. Here we plot electron energy in drive and main bunches versus distance from the head of the drive bunch at the accelerator location of 18 m downstream from the accelerator entrance. The inset in the middle shows current in the drive and main bunches, and the wakefield produced by the drive bunch with this current distribution. It is approximately at this location that some tail electrons in the drive bunch begin to be accelerated by the wake produced by head electrons. In this simulation Gaussian distribution in the main bunch was used. A combination of the main bunch self-wakefield and the drive bunch wakefield produce a noticeable correlated energy variation along the main bunch. However, this energy variation can be tolerated in the FEL, as shown later. Calculations show that the main bunch with an inverse triangular current distribution proposed in [31] will have the self-wakefield canceling the drive bunch wakefield and significantly reduced correlated energy variation.

The straightness of the beam trajectory in the quadrupole wiggler is critical for maintaining the beam stability. Preliminary simulations point out that it should be at a micrometer level. This requirement presents significant challenges, but is feasible in principle, as demonstrated in dipole undulators of modern FELs.

ISBN 978-3-95450-133-5

FEL CONSIDERATIONS

Results of particle tracking for a main beam presented above and a particle distribution obtained there were used as an input particle distribution for modelling of the self-amplified spontaneous emission (SASE) process in the undulator line. Undulator parameters and other key parameters of this modelling are given in Table 3.

Table 3: SASE FEL Parameters

Parameter	Value	Units
Undulator period	1.8	cm
Undulator parameter, K	1.0	
Main beam mean energy	1.88	GeV
Main bunch charge	250	pC
Main bunch peak current	3	kA
Normalized emittance	1	μm
Main bunch relative energy spread, rms	0.3	%
FEL Pierce parameter, ρ	0.01	
X-ray wavelength	1	nm
X-ray peak power*	5	GW
FWHM x-ray pulse bandwidth, $\Delta\omega/\omega$	3.8	%

* averaged over the x-ray pulse length

Plots in Figure 8(a)-(d) show (a) the peak current and electron energy distribution in the main bunch, (b) the nonlinear saturation of SASE FEL gain in approximately 20 gain lengths, (c) peak x-ray power after the saturation, and (d) the x-ray spectrum. The slice energy spread of the electron beam is less than the FEL Pierce parameter ρ and no undulator tapering is used. However an additional undulator with tapering can be used beyond the saturation to increase the output power by a factor of 3 to 5.

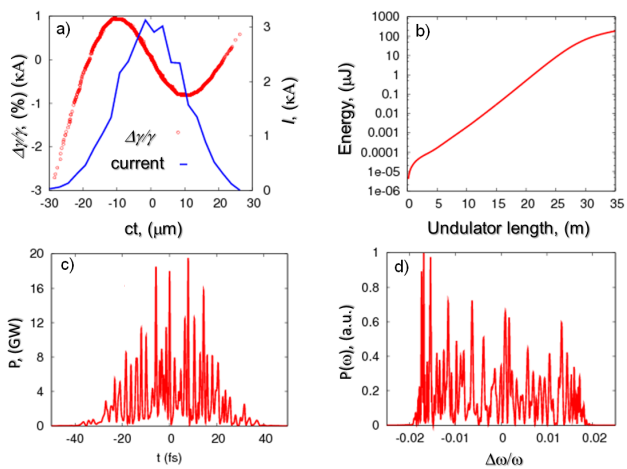

Figure 8: Current and energy distribution of the main bunch (a) and results of the FEL modeling described in the text (b)-(d).

Some applications may not be able to use FEL output with large frequency spread as in the above case, while others may benefit from it. For example, the time-resolved x-ray Laue diffraction actually requires a relatively large spectral bandwidth. A more ambitious plan would use a soft-x-ray self-seeding similar to one presented in [32] to obtain a narrow bandwidth radiation with significantly increased peak power. The feasibility of this option is yet to be determined in future studies.

CONCLUSION

It has been shown that the collinear wakefield accelerator is a viable candidate to be used in a synchrotron light source facility with multiple FELs. The accelerator is reasonably compact, flexible, and can support the FEL producing up to $5\text{x}10^4$ x-ray pulses per sec. The entire facility can consist of up to ten independent FELs, each with its own collinear wakefield accelerator. The emphases have been given to finding regimes with stable beam operation at a high bunch repetition rate. The important component of the collinear wakefield accelerator is a quadrupole wiggler that allows suppression of the single-bunch breakup instability using BNS damping. Maintaining straightness of the beam trajectory through the wiggler at a few micrometer level presents significant challenges, but is feasible in principle. While we focused here on round structures, note however that flat geometries both for corrugated and dielectric structures were also proposed [33,34] that may offer specific advantages for a practical realization of the CWA. For example, the quadrupole wakefield, that is present in the planar geometry, may actually help to improve beam stability.

The strawman FEL facility design considered here only establishes the feasibility of this approach, but leaves many questions for future R&D.

REFERENCES

[1] P. Emma et al., "First lasing and operation of an ångstrom-wavelength free-electron laser," *Nat. Photonics*, vol. 4, pp. 641-647, Aug. 2010.

[2] W. Ackermann et al., "Operation of a free-electron laser from the extreme ultraviolet to the water window," *Nat. Photonics*, 1, 336-442, Jun. 2007.

[3] T. Ishikawa et al., "A compact X-ray free-electron laser emitting in the sub-ångström region," *Nat. Photonics*, vol. 6, pp. 540-544, Feb. 2012.

[4] E. Allaria et al., "Highly coherent and stable pulses from the FERMI seeded free-electron laser in the extreme ultraviolet," *Nat. Photonics*, vol. 6, pp. 699-704, Aug. 2012.

[5] J. Corlett et al., "A Next Generation Light Source Facility at LBNL," *Proceedings of 2011 Particle Accelerator Conference,* New York, NY, 2011, pp. 775-777.

[6] I. Blumenfeld et al., "Energy doubling of 42 GeV electrons in a metre-scale plasma wakefield accelerator," *Nature*, vol. 445, pp. 741-744, Feb. 2007.

ISBN 978-3-95450-133-5

[7] M. C. Thompson et al., "Breakdown Limits on Gigavolt-per-Meter Electron-Beam-Driven Wakefields in Dielectric Structures," *Phys. Rev. Lett.,* vol. 100, no. 21, pp. 214801, May 2008.
[8] G. A. Voss and T. Weiland, "Particle Acceleration by Wake Field", DESY report M-82-10, April 1982.
[9] K. L. F. Bane, P. Chen, P. B. Wilson, "On collinear wake field acceleration", SLAC - PUB – 3662, April 1985.
[10] H. Figueroa et al. "Direct Measurement of Beam-Induced Fields in Accelerating Structures." *Phys. Rev. Lett.*, vol 60, 2144, 1988.
[11] W. Gai et al. Experimental Demonstration of Wake-Field Effects in Dielectric Structures. *Phys. Rev. Lett.*, vol 61, 2756, 1988.
[12] C.K. Sinclair. *Nuclear Instruments and Methods in Physics Research A*, vol 557, p. 69 (2006).
[13] Jing et al., "High Power Testing of a Fused Quartz-Based Dielectric- Loaded Accelerating Structure", SLAC-PUB-12958, 2007.
[14] D. Shchegolkov and E. Simakov, "Design of an emittance exchanger for production of special shapes of the electron beam current," *Phys. Rev. ST Accel. Beams*, vol. 17, pp. 041301, Apr. 2014.
[15] M. Cornacchia and P. Emma, "Transverse to longitudinal emittance exchange," *Phys. Rev. ST Accel. Beams*, vol. 5, pp. 084001, Aug. 2002.
[16] P. Emma et al., "Transverse-to-longitudinal emittance exchange to improve performance of high-gain free-electron lasers," *Phys. Rev. ST Accel. Beams*, vol. 9, pp. 100702, Oct. 2006.
[17] B. Jiang et al., "Emittance-Exchange-Based High Harmonic Generation Scheme for a Short-Wavelength Free Electron Laser," *Phys. Rev. Lett*., vol. 106, no. 11, pp. 114801, Mar. 2011.
[18] Y.–E. Sun, et al., "Tunable Subpicosecond Electron-Bunch-Train Generation Using a Transverse-To-Longitudinal Phase-Space Exchange Technique," *Phys. Rev. Lett*., vol. 105, no. 23, pp. 234801, Dec. 2010.
[19] P. Piot et al., "Generation of relativistic electron bunches with arbitrary current distribution via transverse-to-longitudinal phase space exchange," *Phys. Rev. ST Accel. Beams*, vol. 14, no. 2, pp. 022801, Feb. 2011.
[20] B. E. Carlsten et al., "Using an emittance exchanger as a bunch compressor," *Phys. Rev. ST Accel. Beams*, vol. 14, no. 2, pp. 084403 Aug. 2011.
[21] D. Xiang and A. Chao, "Emittance and phase space exchange for advanced beam manipulation and diagnostics," *Phys. Rev. ST Accel. Beams*, vol. 14, no. 11, pp. 114001, Nov. 2011.
[22] G. Andonian, "Bunch profile shaping using beam self-wakefields in a dielectric structure" *Proceedings of the 16th Advanced Accelerator Concepts Workshop*, to be published.
[23] A. Zholents and M. Zolotorev, "A New Type of Bunch Compressor and Seeding of a Short Wave Length Coherent Radiation," ANL/APS/LS-327, (May 2011)
[24] G. Ha et al., "Start-to-end beam dynamics simulation of double triangular current profile generation in Argonne Wakefield Accelerator," Advanced Accelerator Workshop, Austin, TX, 2012, pp. 693-698.
[25] J. G. Power et al., "Longitudinal Bunch Shaping with a Double Dogleg based Emittance Exchange Beam Line," Proceedings of IPAC2014, Dresden, Germany, 2014 pp. 1506-1508.
[26] A. Chao, "Instabilities in Linear Accelerators," in *Physics of collective beam instabilities in high energy accelerators*, New York: Wiley & Sons, 1993, ch. 3, pp. 127-160.
[27] W. Gai et al., "Numerical simulations of intense charged-particle beam propagation in a dielectric wake-field accelerator," *Phys. Rev. E*., vol. 55, no. 3 pp. 3481-3488, Mar. 1997.
[28] V. Balakin et al., "VLEPP: Transverse Beam Dynamics," *Proceedings of the 12th International Conference on High Energy Accelerators*, Fermi National Acceleratory Laboratory, Batavia, IL, 1983, p. 119.
[29] C. Li et. al., "High Gradient Limits due to Single Bunch Beam Breakup in a Collinear Dielectric Wakefield Accelerator," *Phys. Rev. ST Accel. Beams,* to be published.
[30] D. Shchegolkov et al., "Suppressing Parasitic Effects in a Long Dielectric Wakefield Accelerator" *Proceedings of the 16th Advanced Accelerator Concepts Workshop*…, to be published.
[31] T. Katsouleas et al., "Beam loading in plasma accelerators," *Particle Accelerators*, vol. 22, pp.81-99, 1987.
[32] D. Ratner et al., "Soft X-ray Self-Seeding Setup and Results at LCLS," *Proceedings of 36th International Free Electron Laser Conference*…, to be published, 2014.
[33] A. Tremaine et al. "Electromagnetic wake fields and beam stability in slab-symmetric dielectric structures", *Phys. Rev. E*, vol 56, p. 7204,1997.
[34] K.Bane, G.Stupakov, "*Impedance of a Rectangular Beam Tube with Small Corrugations*", *Phys. Rev. ST Accel. Beams*, vol 6, 024401, 2003

ISBN 978-3-95450-133-5